Title
Large earthquakes create vertical permeability by breaching aquitards

Journal
Water Resources Research, 52(8)

ISSN
0043-1397

Authors
Wang, Chi-Yuen
Liao, Xin
Wang, Lee-Ping
et al.

Publication Date
2016-08-01

DOI
10.1002/2016wr018893

Peer reviewed

Large earthquakes create vertical permeability by breaching aquitards

Chi-Yuen Wang[1], Xin Liao[1,2], Lee-Ping Wang[3], Chung-Ho Wang[4], and Michael Manga[1]

[1] Department of Earth and Planetary Science, University of California, Berkeley, California, USA,

[2] Institute of Disaster Prevention, Beijing, China,

[3] Department of Chemistry, University of California, Davis, California, USA, 4 Academia Sinica, Nankang, Taipei, Taiwan

Abstract

Hydrologic responses to earthquakes and their mechanisms have been widely studied. Some responses have been attributed to increases in the *vertical* permeability. However, basic questions remain: How do increases in the vertical permeability occur? How frequently do they occur? Is there a quantitative measure for detecting the occurrence of aquitard breaching? We try to answer these questions by examining data from a dense network of ~50 monitoring stations of clustered wells in a sedimentary basin near the epicenter of the 1999 M7.6 Chi-Chi earthquake in western Taiwan. While most stations show evidence that confined aquifers remained confined after the earthquake, about 10% of the stations show evidence of coseismic breaching of aquitards, creating vertical permeability as high as that of aquifers. The water levels in wells without evidence of coseismic breaching of aquitards show tidal responses similar to that of a confined aquifer before and after the earthquake. Those wells with evidence of coseismic breaching of aquitards, on the other hand, show distinctly different postseismic tidal response. Furthermore, the postseismic tidal response of different aquifers became strikingly similar, suggesting that the aquifers became hydraulically connected and the connection was maintained many months thereafter. Breaching of aquitards by large earthquakes has significant implications for a number of societal issues such as the safety of water resources, the security of underground waste repositories, and the production of oil and gas. The method demonstrated here may be used for detecting the occurrence of aquitard breaching by large earthquakes in other seismically active areas.

1 Introduction

Most groundwater systems are, to a first approximation, horizontally or subhorizontally layered. The average horizontal permeability is thus dominated by the most permeable layers. In contrast, the average vertical permeability is limited by the least permeable layers, and may be many orders of magnitude lower than the average horizontal permeability [e.g., *Ingebritsen et al*., 2006]. As a consequence, groundwater flow is typically horizontal through the most permeable beds, i.e., the aquifers, and confined by the relatively impermeable beds, i.e., the aquitards.

Permeability can be altered by the stresses produced by earthquakes. *Rojstaczer et al*. [1995] used a model of horizontal flow to interpret the changes in stream discharge after the 1989 M6.9 earthquake in California and to infer that permeability of aquifers increased over regional scales. Analyses of the tidal response of water level in wells confirm that large earthquakes can locally change the permeability of aquifers [e.g., *Elkhoury et al*., 2006; *Xue et al*., 2013; *Shi et al*., 2015; *Lai et al*., 2016]. These latter studies also used a model of horizontal flow [e.g., *Hsieh et al*., 1987] to interpret the tidal data and to infer changes of permeability in the horizontal direction.

Coseismic increase of the vertical permeability was inferred earlier from stream flow increases in Taiwan following the 1999 M7.6 Chi-Chi earthquake [*Wang et al*., 2004a] and in California following the 2003 M6.5 San Simeon earthquake [*Wang et al*., 2004b] and the 2014 M6.0 South Napa earthquake [*Wang and Manga*, 2015]. These studies, however, do not provide quantitative information on how common are the postseismic increase of the vertical permeability or how long such increases may persist. In this study we look for answers to these questions by examining water levels in closely spaced wells (clustered wells) open to different aquifers. Such data are generally difficult to obtain because large earthquakes rarely occur near clustered wells with good water level data. An exceptional case occurred in western Taiwan where an alluvial fan, monitored with a dense and evenly distributed network of clustered wells (Figure 1), was located near the epicenter of the 1999 M7.6 Chi-Chi earthquake. Analysis of water levels in these clustered wells allows us to assess whether such changes are common and how the changes evolve over time.

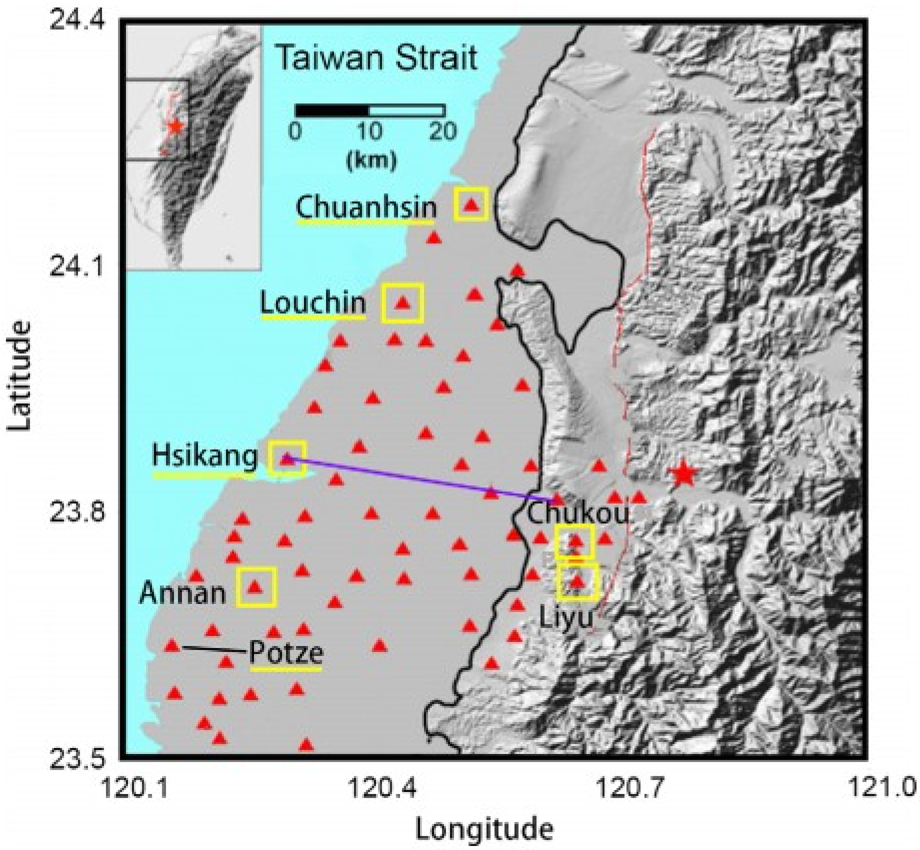

Figure 1. Topographic map of western central Taiwan showing the western foothills of the Taiwan mountains, the Choshui Alluvial Fan, and the locations of hydrological stations with clustered wells (red triangles). Yellow squares show stations with postseismic convergence of water levels among different confined aquifers; underlined names identify stations with lithologic well logs shown in Figure 2b and considered in detail in this study. Red star shows the epicenter of the Chi-Chi earthquake; broken red curves show the traces of the ruptured fault; purple line shows the location of the cross section in Figure 2a.

In addition, we compare the tidal response of water level in wells that showed evidence of an increased vertical permeability after the earthquake with those that did not. In wells that showed *no* evidence of coseismic increase of the vertical permeability, the tidal response of aquifers before and after the earthquake remains along the trend defined by a confined aquifer model. In wells that showed evidence of coseismic increase of the vertical permeability, on the other hand, the tidal response of aquifers immediately after the earthquake was distinctly different from that before the earthquake and fell away from the trend defined by a confined aquifer. Furthermore, the tidal response also shows that wells in a cluster with postseismic convergence of water levels became hydraulically connected after the earthquake, and that the connection lasted many months after the groundwater level returned to the preseismic levels.

2 Previous Studies

Postseismic increases in stream flow are widely reported but the mechanism remains debated. Proposed hypotheses include earthquake-induced static strain in aquifers [*Muir-Wood and King*, 1993], enhanced permeability [*Briggs*, 1991; *Rojstaczer and Wolf*, 1992; *Rojstaczer et al*., 1995], consolidation and/or liquefaction of unconsolidated sediments [*Roeloffs,* 1998; *Manga*, 2001; *Manga et al*., 2003], enhanced vertical permeability [*Wang et al*., 2004a], expulsion of hydrothermal water from depth [*Wang et al*., 2004b], and water shaken out of the vadose zone [*Manga and Rowland*, 2009; *Mohr et al*., 2015]. *Rojstaczer et al*. [1995] pointed out that the static strain hypothesis requires the expulsion of pore water from >10 km thick crust, which is inconsistent with the observed time-history of the increase of stream flow or the composition and temperature of the stream water. *Manga et al*. [2003] showed that the base flow recession stayed constant after several earthquakes, implying that horizontal hydraulic diffusivity did not change. *Wang et al*. [2004a] showed that after the 1999 Chi-Chi earthquake in Taiwan, coseismic increases in stream flow occurred in streams with headwater in the nearby foothills with little sedimentary cover, but did not increase in streams that originated on the alluvial fan. This observation contradicts the consolidation-liquefaction hypothesis that would predict the sediment-rich alluvial fan to be the source of the increased flow. Instead, the observation suggests that the extra water may have been released from the foothills and an increased vertical permeability allowed the released water to rapidly discharge to the streams [*Wang et al*., 2004a]. The model of coseismic increase of the vertical permeability has been used successfully in simulating increased stream flow after several large earthquakes [e.g., *Wang et al*., 2004b; *Manga and Rowland*, 2009]. It is also consistent with the observation that the recession constant does not change after earthquakes because evaluation of the recession constant depends only on the horizontal permeability [e.g., *Wang and Manga*, 2010]. Following the 2014 M6.0 South Napa earthquake in California, several dry streambeds started to flow. The compositions of the oxygen and hydrogen isotopes in the pristine emergent water showed that it originated from meteoric water precipitated in the nearby mountains, consistent with the hypothesis of an increased vertical permeability that allowed rapid recharge of the aquifers that discharge to the streams [*Wang and Manga*, 2015].

Groundwater temperature may also be used as a tracer to study earthquake-induced changes in groundwater flow [e.g., *Mogi et al*., 1989]. Groundwater temperature across a large alluvial fan showed systematic, basin-wide changes following the Chi-Chi earthquake, from about −1°C near the foothills to about +1°C near the coast [*Wang et al*., 2013]. Temperature of thermal springs in the Southern Alps, New Zealand, also showed a decrease of ~1°C following the 2009 Mw7.8 Dusky Sound (Fiordland) and the 2010 Mw7.1

Darfield (Canterbury) earthquakes [*Cox et al*., 2015]. Simulation of the groundwater flow and heat transport after the Chi-Chi earthquake to explain the basin-wide temperature change showed that an increase of the vertical permeability by a factor of >10^2 to a depth of ~4 km may be required to explain the observations [*Wang et al*., 2013].

Liao et al. [2015] studied the change of tidal response of water level in a ~4 km well in western China and showed that the 2008 M7.8 Wenchuan earthquake changed the poroelastic properties of the groundwater system, in addition to the permeability of the aquifer. The finding is consistent with the hypothesis that large earthquakes may breach aquitards in groundwater systems to depths of several km. Finally, the migration of seismic swarms was used to infer increases of the vertical permeability at depths of ~20 km [e.g., *Ingebritsen and Manning*, 2010; *Ingebritsen et al*., 2015] assuming that the migration of seismic swarms reflects the diffusion of pore pressure.

3 Geologic Setting

The island of Taiwan is the product of the collision between the Eurasian Plate and the Philippine Sea Plate in the late Cenozoic. The prevailing structure is a N-S elongated mountain belt bordered on the west by the Western Foothills and the Coastal Plain that, in turn, is bordered on the west by the Taiwan Strait (Figure 1). The Choshui Alluvial Fan, with an area of ~1800 km^2, is part of the Coastal Plain. A network of evenly distributed hydrological stations was installed on this fan in the early 1990s for monitoring water resources (Figure 1). At each station, one to five wells were drilled to depths from 24 to 306 m, each opened to a distinct aquifer and instrumented with piezometers that record groundwater level hourly with a precision of 1 mm. About 50 stations were functioning at the time of the Chi-Chi earthquake, providing unprecedented data for the response of groundwater in clustered wells to a large earthquake in the near field.

A simplified E-W hydrogeologic cross section of the Choshui Alluvial Fan is shown in Figure 2a; detailed lithologic logs at the stations analyzed in this study are given in Figure 2b. These stations are chosen to illustrate the various responses of wells to the earthquake and to tides; i.e., two wells at the Chuanhsin Station showed both postseismic convergence of water levels and good tidal response (Figures 7a, 7c, and 10); two wells at the Hsikang Station (Figure 3) and two at the Louchin Station (Figures 7b and 7d) showed postseismic convergence of water levels but poor tidal response; wells at the Potse Station showed no postseismic convergence of water levels but good tidal response (Figure 6).

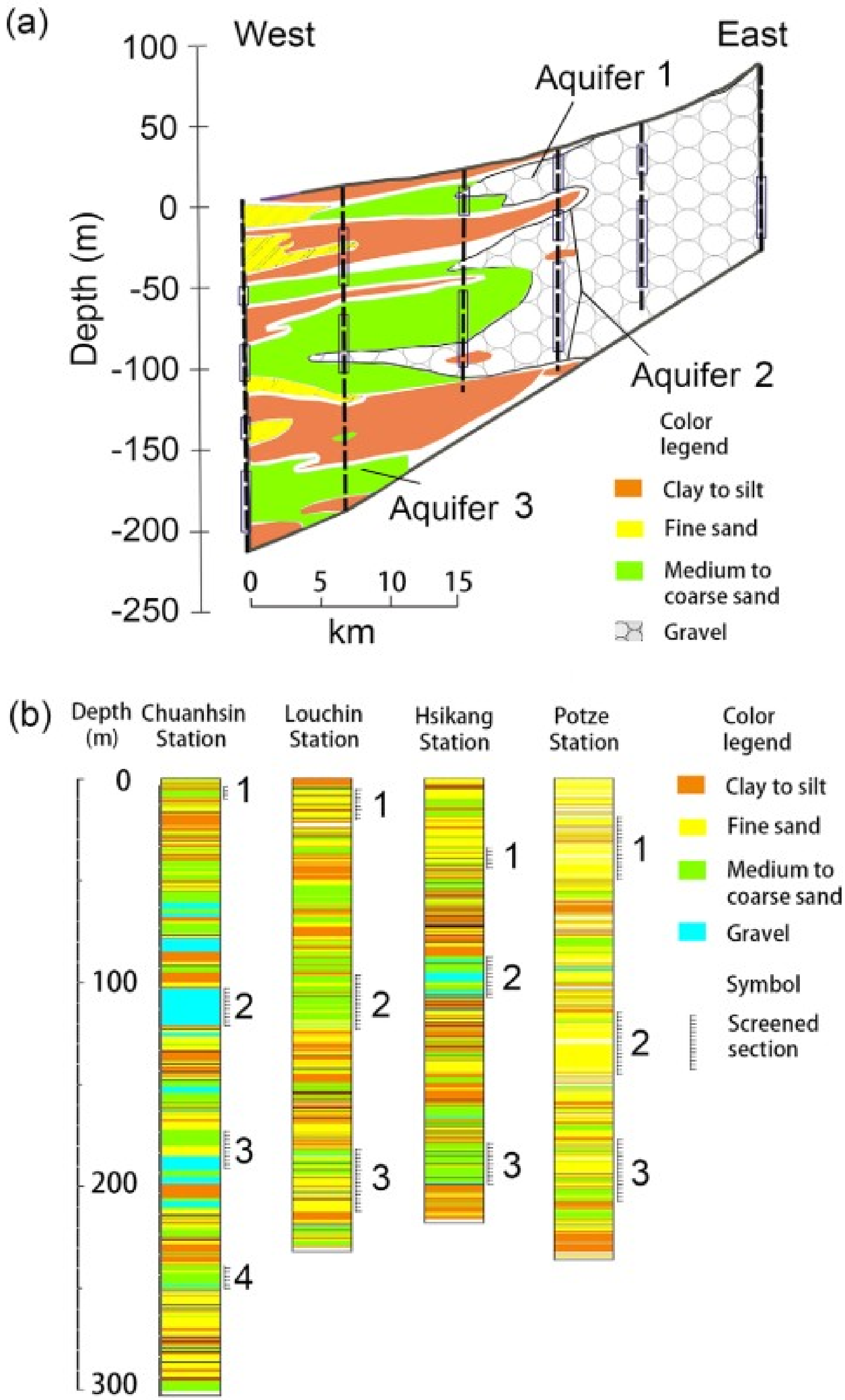

Figure 2. (a) Simplified E-W hydrogeologic cross section of the Choshui Alluvial Fan reconstructed from well logs close to the purple line in Figure 1. (b) Lithologic logs for the four stations discussed in detail in this paper (Figure 1 for locations). Multiple screened sections of aquifers are numbered sequentially from top down; barbed lines show the locations of screens. Note that these stations are not located along the cross section shown in Figure 2a.

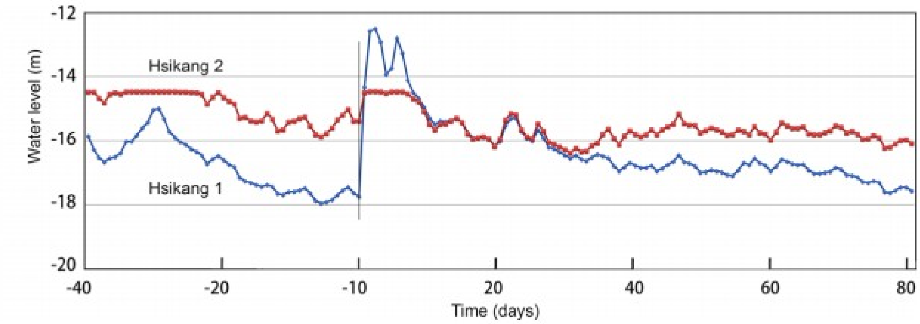

Figure 3. Daily average of water levels in two wells at the Hsikang Station (see Figure 1 for location) before and after the Chi-Chi earthquake, recorded by piezometers located at depths of 40 m (Hsikang 1) and 99 m (Hsikang 2), respectively. Water level is referenced to the mean sea level, with positive values above sea level and negative values below sea level. Time of the earthquake is marked by a vertical line at t = 0. Positive numbers are days after the earthquake and negative numbers are days before the earthquake. The wells are open to aquifers separated by an aquitard ~40 m thick (see Figure 2b for lithology and screen depths).

The alluvial fan consists of unconsolidated Holocene and Pleistocene sediments. Massive gravel beds accumulated in the proximal section of the fan near the exit of the Choshui River from the foothills. Away from the proximal section toward the coastal plain, sediments become finer and grade into layers of sand and marine mud. Reconstruction of the subsurface structures [*Jiang et al*., 1999] based on well logs show several distinct aquifers away from the proximal area (Figure 2a). The uppermost aquifer is partially confined; the lower ones are confined. Beneath the alluvial fan is a basement of consolidated but highly cracked Cenozoic sedimentary rocks.

4 Results

4.1 Postseismic Convergence of Water Levels

During the Chi-Chi earthquake, water levels in most wells on the alluvial fan rose [*Chia et al*., 2008; *Wang et al*., 2001], which was attributed to coseismic undrained consolidation of sediments by seismic shaking [*Wang et al*., 2001]. At most well clusters, water levels in different wells remained distinct after the earthquake, showing that the aquifers remained confined. However, a significant number of stations (Figure 1), about a tenth of the total number of working stations, showed postseismic convergence of water levels in different aquifers. Figure 3 shows one such example, where water levels in two wells at the Hsikang Station (see location in Figure 1) were different by ~2 m before the earthquake, but both rose and converged to the same level 10 days after the earthquake, and stayed converged for about 30 days. Afterward, water levels in the two wells started to diverge and reached the preseismic difference in ~4 months (not shown).

We may obtain an order-of-magnitude estimate of the postseismic vertical permeability from the time required for the water levels in the two wells to converge and the thickness of the intervening aquitard. Assuming Darcy's law for the postseismic vertical flow in the aquitard between the aquifers and solving the one-dimensional flow equation under appropriate boundary condition [*Wang et al*., 2004c], we find the relationship between the characteristic time τ for the flow and the hydraulic diffusivity κ_v of the confining layer between the aquifers, which largely controls the vertical permeability of the groundwater system

$$\tau \sim \frac{4h^2}{\kappa_v \pi^2}, \quad (1)$$

where κ_v is related to the vertical permeability (k_V) by $\kappa_v = (\rho g k_V)/\mu S_s$, h is the thickness of the aquitard between the two aquifers, S_s the specific storage of the aquifer, ρ and μ are, respectively, the density and viscosity of water, and g the gravitational acceleration. The lithology well log at the Hsikang Station (Figure 2b) shows $h \sim 40$ m; thus, for $\tau \sim 10$ days, we have $\kappa_v \sim 10^{-3}$ m^2/s, which is equivalent to k_V ranging from 10^{-16} to 10^{-14} m^2 for a reasonable range of S_s from 10^{-6} to 10^{-4} m^{-1}. This range of k_V is close to the lower limit of permeability normally associated with aquifers [e.g., *Fetter*, 2001].

Figures 4a and 4b show water level convergence at two other stations in a different manner from that at the Hsikang Station. Different wells at each of the Chuanhsin and Louchin Stations (see Figure 1 for location) showed distinct water levels before the Chi-Chi earthquake. During the earthquake, water levels in different wells rose and then converged to the same level within 2–5 h after the earthquake (Figures 4a and 4b). The rapid convergence suggests large coseismic increases in the vertical permeability between aquifers.

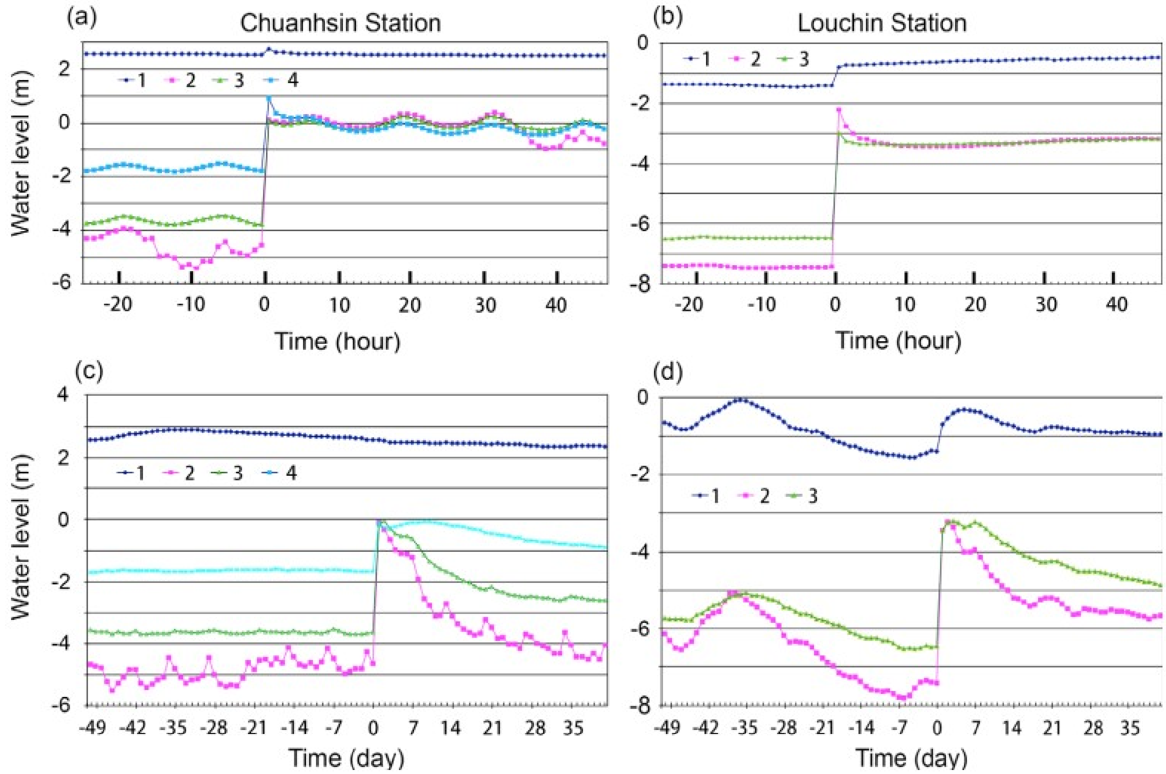

Figure 4. Water levels at two stations before and after the Chi-Chi earthquake. Water level is referenced to the mean sea level, with positive values above sea level and negative values below sea level. (a) Hourly data for water level in four wells at the Chuanhsin Station documented by piezometers located, respectively, at depths of 8 m (aquifer 1), 111 m (aquifer 2), 181 m (aquifer 3), and 245 m (aquifer 4). Time of earthquake is marked by t = 0. The wells are open to aquifers separated by aquitards 40–50 m thick (see Figure 2b for lithology and screen depths). (b) Hourly data for water level in three wells at the Louchin Station documented by piezometers located, respectively, at depths of 12 m (aquifer 1), 110 m (aquifer 2), and 199 m (aquifer 3). Time of earthquake is marked by t = 0. The wells are open to aquifers separated by an aquitard ~60 m thick (see Figure 2b for lithology and screen depths). Notice that the water levels at each station were separated before the Chi-Chi earthquake, but converged rapidly after the earthquake. (c, d) Daily average of water levels at the same two stations.

We may also obtain an order-of-magnitude estimate of the postseismic vertical permeability at these stations, following the procedure used above for the Hsikang Station. Referring to Figure 2b we find h ~ 40 m at the Chuanhsin Station and ~60 m at the Louchin Station; for τ of 2 and 5 h at these stations, respectively, k_V ranges from 10^{-14} to 10^{-12} m^2 at both stations for a range of S_s from 10^{-6} to 10^{-4} m^{-1}. This range of k_V is similar to that normally associated with aquifers [e.g., *Fetter*, 2001]. In other words, the vertical permeability of the breached aquitards increased to values as high as that of aquifers.

Other cases of postseismic convergence of water levels are shown in Supporting Information. Such postseismic convergence of water levels is unlikely to have occurred by chance, because the probability for independent aquifers to generate excess pore pressure by seismic shaking to reach the same level, and stay at the same level for an extended time, is exceptionally small. It is more likely that the formerly isolated aquifers became hydraulically connected by conductive paths (e.g., cracks) after the earthquake so that they showed the same elevated pressure. The different amount of time required for water levels in different wells to reach the same level after the earthquake may reflect different vertical permeability of the breached aquitard between aquifers.

It is notable that water levels at the Chuanhsin Station and the Louchin Station stayed converged for only about 2 days (Figures 4c and 4d), while those at the Hsikang Station stayed converged for almost a month before starting to diverge. *Brodsky et al*. [2003] proposed gradual reclogging of seismically unclogged cracks by precipitates or colloidal particles as a mechanism for the postseismic return of groundwater level to preearthquake values. In this model the different amount of time for the water levels to remain converged may reflect differences in the time required to reclog the cracks connecting the aquifers. *Wang et al*. [2004c] interpreted the postseismic return of groundwater level to preseismic levels by lateral flow to local discharge areas, such as a stream. In this model the different amount of time for water levels to remain converged may reflect different horizontal permeability and/or different distances to the local discharge area that controls the equilibrium postseismic groundwater level.

4.2 Tidal Analysis

We can test the above model of coseismic increase of vertical permeability by comparing the postseismic tidal responses of clustered wells. The model predicts that the tidal responses of different aquifers that are different before the earthquake become similar after the earthquake if they become hydraulically connected. Suitable wells, however, are difficult to find because we require both postseismic convergence of water levels and good tidal responses. Of all the wells that showed a postseismic convergence of water levels, only two at the Chuanhsin Station had good tidal signals (Figure 4a).

The wells on the Choshui Alluvial Fan with good tidal signals are all located near the coast of the Taiwan Strait that is a laterally confined, shallow (~60 m) seaway. Ocean tides are expected to be the dominant source of the tidal signals in these wells. Tide gauge data were not available at the time of the Chi-Chi earthquake. However, more recent studies [e.g., *Jan et al*., 2004] show that tides in the Taiwan Strait are dominated by the semidiurnal M2 tides that originate in the East China Sea to the north of the strait. The southward propagating tides are amplified by shoaling and narrowing in the strait and reach an amplitude of 1.8 m near the coast of the Choshui Alluvial Fan [e.g., *Jan et al*., 2004].

The intent of the present study is to compare the relative change in tidal response between different aquifers before and after the Chi-Chi earthquake rather than to interpret the absolute tidal amplitude or phase shift for the determination of aquifer permeability or storage. For this purpose a detailed knowledge of the ocean tide is not required. We use the program Baytap08 (Supporting Information) [*Tamura et al*., 1991] to extract and analyze the tidal signals in water level in clustered wells. The program uses a Bayesian modeling procedure to analyze time series subjected to the constraints of known tidal periods. The time series for the local barometric pressure is included along with the water level data for correcting the barometric effect on water level. We apply a sliding window to the time series to examine the time-dependent variation of the tidal response. The choices of the sliding window and the overlap between successive windows are somewhat arbitrary and we discuss the effect of different choices of sliding window and overlap in Supporting Information. For the present study we choose window lengths of 30–31 days and overlaps of 23–28 days.

As an example of the studied data, we show in Figure 5a the time series of water level in Well 4 at the Chuanhsin Station from April 1 to 22 August 1999. The figure shows, from top down, the original time series of water level, the drift (a long-period component of the time series) [*Agnew and Tamura*, 2008], the tidal component of the time series used in the analysis, and the residual. The tidal signal is strong and suitable for analysis; the residual shows little temporal correlation, as it should. The power spectrum of the drift, shown in Figure 5b, exhibits high-frequency harmonics that could be produced by nonlinear processes such as bottom friction produced by the shallow Taiwan Strait on the southward propagating tides [*Zahel*, 1997].

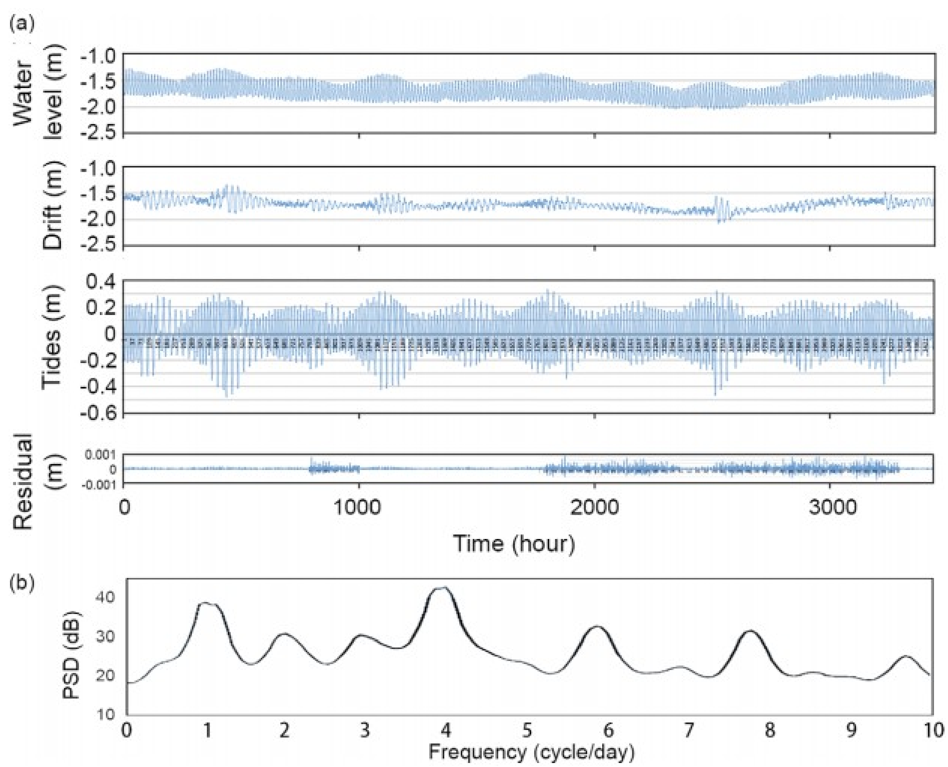

Figure 5. (a) Time series at the Chuanhsin Station, Well 4, from 1 April to 22 August 1999, showing, from top to bottom, original data for water level, drift that was removed before analysis, tidal component used in the analysis, and residual. In this analysis we used a window length of 31 days and an overlap of 28 days. Water level is referenced to the mean sea level, with positive values above sea level and negative values below sea level. (b) Power spectrum of the drift of the time series.

Analysis was made for the tidal components Q1, O1, M1, S1, J1, OO1, 2N2, N2, M2, L2, S2, M3, where S1 and S2 are solar tides affected by the thermal radiation and barometric tides; Q1, O1, M1, J1, OO1, 2N2, N2, L2, and M3 have small signal-to-noise ratios. We use the M2 tide because it has the largest amplitude as well as large signal-to-noise ratio.

4.3 Phase and Amplitude of the Tidal Response

We first examine the phase and amplitude of the tidal response at a station where water levels did *not* converge after the Chi-Chi earthquake. Figure 6 shows the response of water level to the M2 tide in Well 3 at the Potse Station (see location in Figure 1) 1 year before and 1 year after the earthquake. A significant coseismic increase in phase (~7°) occurred at the time of the earthquake, but little change occurred in amplitude, in agreement with the results of previous studies [e.g., *Elkhoury et al*., 2006; *Xue et al*., 2010; *Shi et al*., 2015; *Lai et al*., 2016].

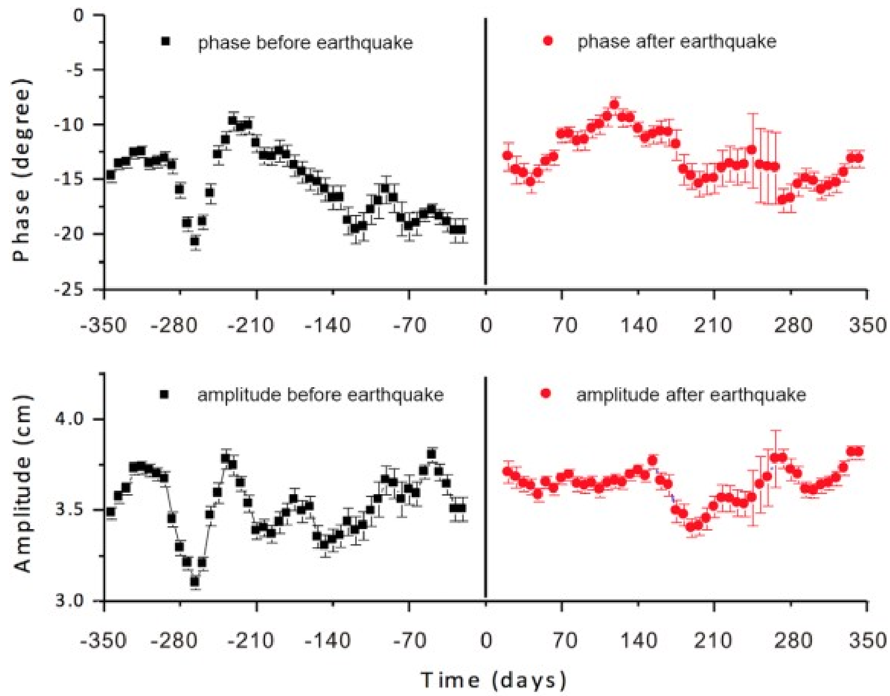

Figure 6. Amplitude and phase shift for water-level response to the M2 tide in Well 3 at Potze Station plotted against time 1 year before and 1 year after the Chi-Chi earthquake (window length of 30 days, overlap of 23 days). Each point represents the amplitude or the phase shift calculated for a data window. Time of the earthquake is marked by a vertical line at t = 0.

In addition to the coseismic change, there are significant time-dependent variations in phase both before and after the earthquake. We interpret this to reflect time-dependent variations of ocean tides in the Taiwan Strait. As noted earlier, the shallow Taiwan Strait (~60 m) may produce frictional drag on the southward propagating tides in the strait. The magnitude of this drag would be modulated by long period tidal disturbances in the open ocean, which in turn would modulate the phase of tides in the strait (Supporting Information).

We next examine the tidal response of stations where postseismic convergence of water level occurred. However, the requirement of post-seismic convergence of water levels, which accounts for only ~10% of all the stations, together with adequate data for tidal analysis from the wells showing such convergence, make the occurrence of such stations rare, at least in the alluvial fan we studied here. The Chuanhsin Station (see Figure 1 for location) fulfills both these requirements. Figure 7 shows the phase response of water level to the M2 tide in Well 3 and Well 4 at the Chuanhsin Station.

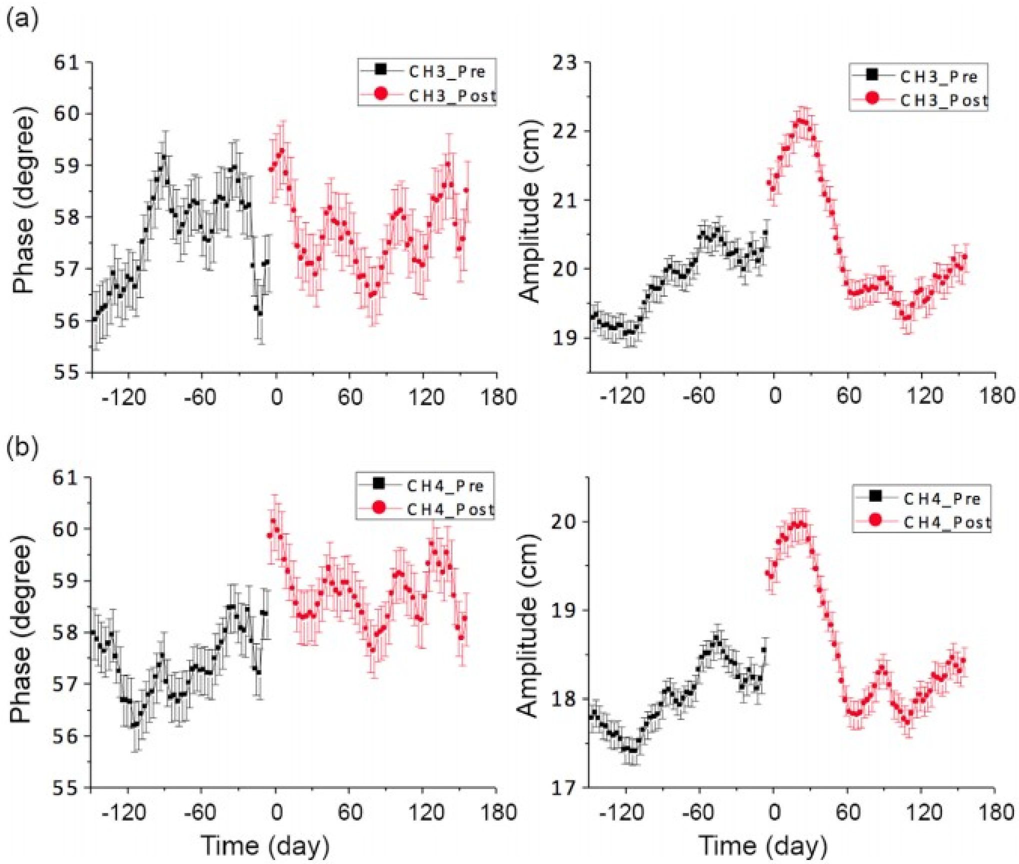

Figure 7. (a) Calculated phase shift and amplitude of the tidal response of water level in Well 3 at the Chuanhsin Station before (black) and after (red) the Chi-Chi earthquake (window length of 31 days, overlap of 28 days). Each point represents the phase shift or amplitude calculated for a data window. (b) Calculated phase shift and amplitude of the tidal response of water level in Well 4 at the Chuanhsin Station before (black) and after (red) the Chi-Chi earthquake.

A distinct feature in the tidal response in both wells at the Chuanhsin Station, as compared with that at the Potze Station, is a large coseismic increase in amplitude that peaked at ~30 days but returned to the pre-seismic level ~60 days after the earthquake. Notice also that before the Chi-Chi earthquake, the time histories of phase shift in the two wells were distinctly different from each other, but became strikingly similar after the earthquake. To further illustrate the change of confinement between the two aquifers, we plot in Figure 8 the phase of M2 tidal response of water level in Well 3 against that in Well 4 before and after the Chi-Chi earthquake. While there was little correlation in the phase response between the two wells before the Chi-Chi earthquake (Figure 8a, $r^2 = 0.00$), there was a strong correlation in phase responses between the two wells after the earthquake (Figure 8b, $r^2 = 0.76$). The postseismic similarity in the tidal response in the two wells supports the hypothesis that the confining layer between the two aquifers was breached and the two aquifers became hydraulically connected after the earthquake. It is also important to note that this similarity in tidal response lasted at least ~6 months after the earthquake, before the data quality deteriorated in Well 3.

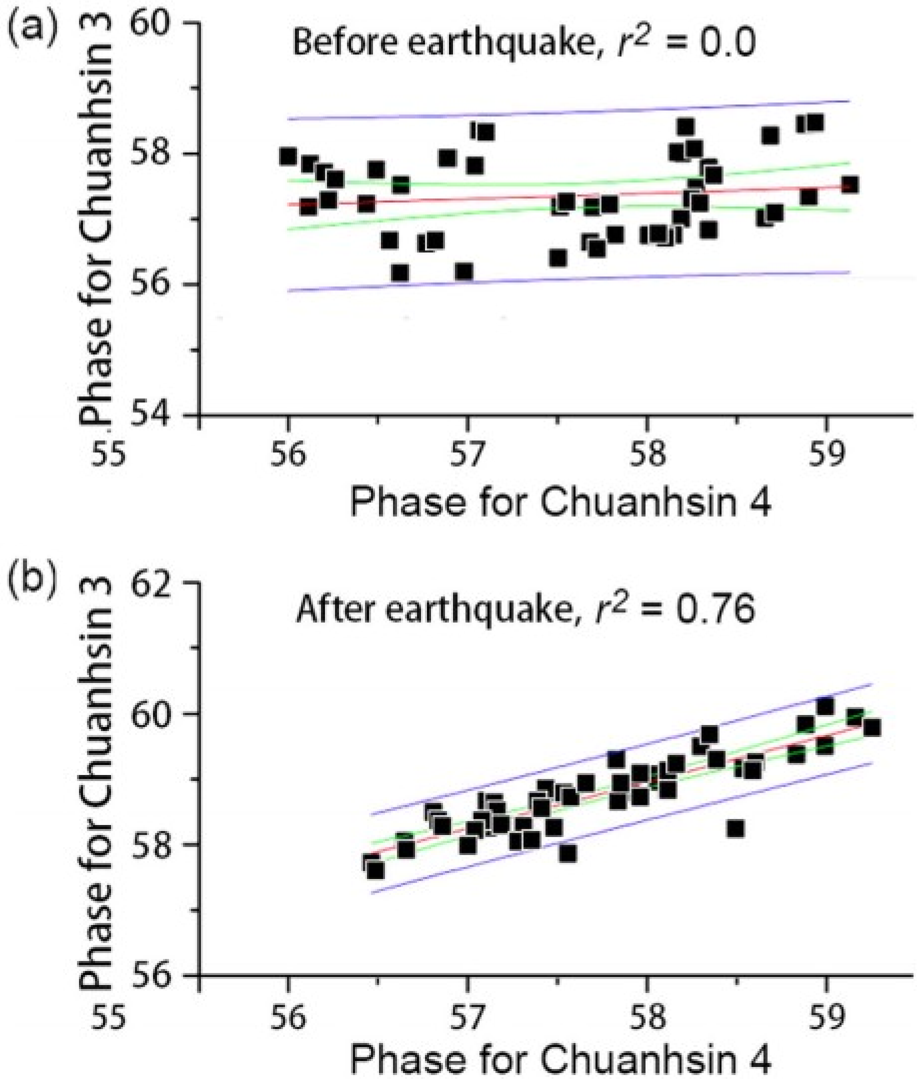

Figure 8. Plots of the phase of M2 tidal response of water level in Well 3 at the Chuanhsin Station against that in Well 4 for all the data presented in Figure 7. (a) Before the Chi-Chi earthquake there is no correlation ($r^2 = 0.00$) between the tidal responses in the two wells. (b) After the Chi-Chi earthquake there is a strong correlation ($r^2 = 0.76$) between the tidal responses in the two wells.

4.4 Tidal Response of a Confined Aquifer

Hsieh et al. [1987] derived a solution for the tidal response of water level in a well that opens to a horizontal, laterally extensive, confined, isotropic, and homogeneous aquifer. This model cannot be used to extract the poroelastic properties from the tidal response in the present case, but it provides the means to differentiate between the tidal response of a breached aquifer from that of an unbreached aquifer, as shown below. In this model, the amplitude

(X) and the phase shift (η) of the tidal fluctuations of water level in wells may be related to aquifer properties by the following relations:

$$X=H\left(E^2+F^2\right)^{-1/2},\quad(2)$$

and

$$\eta=-\tan^{-1}(F/E),\quad(3)$$

where H is the amplitude of the tidal fluctuations of the pressure head in the aquifer, and E and F are defined as, respectively,

$$E\approx 1-\left(\omega \mathrm{r_c}^2/2\mathrm{T}\right)\ \mathrm{Kei}\ (\alpha_w),$$

$$F\approx\left(\omega \mathrm{r_c}^2/2\mathrm{T}\right)\ \mathrm{Ker}\ (\alpha_w),$$

where ω is the tidal frequency, Ker and Kei, respectively, are the zeroth-order Kelvin functions, $\alpha_w = (\omega S/T)^{1/2}\, r_w$, T and S, respectively, are the transmissivity and storativity of the aquifer, r_w and r_c are, respectively, the radius of the well and the inner radius of well casing, and transmissivity is related to aquifer permeability (k) through the relation $T = (b\,\rho g k)/\mu$, where b is the thickness of the aquifer, ρ and μ are, respectively, the density and viscosity of water, and g the gravitational acceleration.

Equations 2 and 3 show that the phase of the tidal response in a well depend on the hydraulic properties T and S; but the amplitude (X) depends not only on T and S but also on H which is related to the volumetric strain ϵ through the following relation [*Wang*, 2000],

$$H=-\frac{BK_u\epsilon}{\rho g},\quad(4)$$

where B is the Skempton's coefficient and K_u the undrained bulk modulus. *Liao et al.* [2015] exploited the latter dependence to show that earthquakes can change not only T and S of a groundwater system but also the poroelastic properties B and K_u.

4.5 Tidal Response of Wells Before and After the Chi-Chi Earthquake

We plot in Figure 9 the calculated amplitude versus phase of the M2 tidal response of water level at the Potze Station. The data points, both before and after the Chi-Chi earthquake, agree with the model of a confined aquifer shown by a dashed line [*Hsieh et al*., 1987]. An arrow connecting the last data point before the Chi-Chi earthquake to the first data point after the earthquake is also nearly parallel to the dashed line. These observations suggest that the aquifer remained confined after the earthquake. In addition, Figure 9 shows that H did not change after the earthquake since the vertical position of the dashed line is sensitive to H [*Liao et al.*, 2015], which in turn implies that BK_u did not change after the earthquake (equation 4).

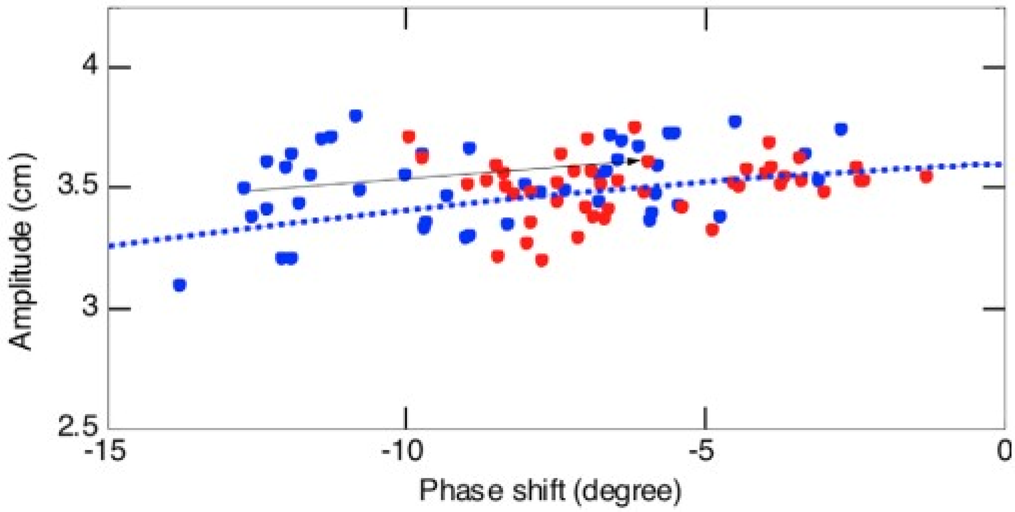

Figure 9. Amplitude plotted against phase shift for water-level response to the M2 tide in Well #2 at Potze Station 1 year before (blue dots) and 1 year after (red dots) the Chi-Chi earthquake. Each point represents the phase shift and amplitude calculated for a data window. The dashed line represents the best fitting model for a confined aquifer [*Hsieh et al.*, 1987], where *S* and *H* are fixed but *T* is allowed to vary. An arrow is drawn from the last point before the Chi-Chi earthquake to the first point after the earthquake, which is nearly parallel to the dashed line.

In Figures 10a and 10b we plot amplitude against phase for the tidal response of water levels in the two wells at the Chuanhsin Station where water levels converged during the Chi-Chi earthquake. Data points before the earthquake show a trend similar to that in Figure 9, consistent with a confined aquifer model (dashed line). After the earthquake, however, data points deviate significantly from the trend defining a confined aquifer. We also connect the last data point before the Chi-Chi earthquake to the first data point after the earthquake with an arrow. The arrows in both diagrams also deviate significantly in direction from the trend defining a confined aquifer (dashed lines), suggesting that the earthquake may have disrupted the confinement of the aquifers. Such postseismic deviation of tidal response from the trend defined by a confined aquifer shows that H, and thus BK_u (equation 4), changed after the earthquake. In other words, the earthquake disrupted the poroelastic properties of the aquifers.

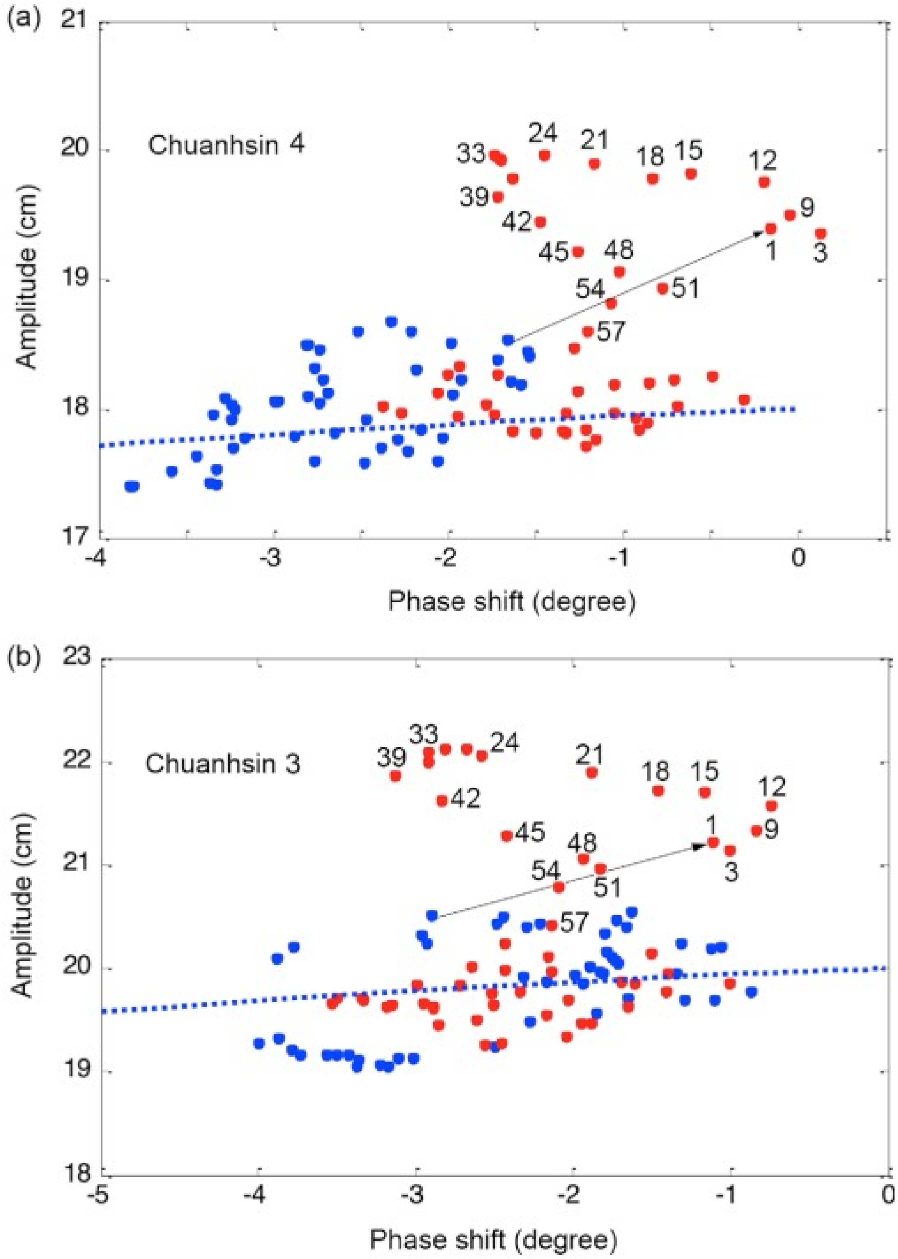

Figure 10. Amplitude versus phase shift for water-level response to the M2 tide in two wells at the Chuanhsin Station. In each well, each point represents the phase shift and amplitude calculated for a data window. Before the earthquake, data points in both wells (blue dots) fit a confined aquifer model (dashed line) [*Hsieh et al.*, 1987]. Coseismic changes in both wells are given by arrows that connect the last preseismic data point to the first postseismic data point. Data points during the first ~60 days after the earthquake are numbered in sequence to show the time-dependent evolution. Both the arrows and the postseismic data points during the first ~60 days after the earthquake deviate significantly from the trend defining a confined aquifer (dashed line), which we refer in the text as the "excursion" from a confined aquifer. Numbering refers to the number of days after the earthquake and the first day in a data window.

We numbered the data points during the first ~60 days after the earthquake in Figures 10a and 10b to highlight the time-dependent excursions from the trend defining a confined aquifer and the similarity between the two wells after the earthquake. The similarity shows that the two aquifers became hydraulically connected after the earthquake.

The termination of the postseismic excursion (Figures 10a and 10b) may give the impression that the groundwater system “healed” in ~60 days after the earthquake. However, Figures 7a and 7b show that the two wells continued to exhibit similar tidal responses long after the first 60 days and this similarity lasted at least ~6 months after the earthquake, before the data quality deteriorated in one of the wells. Thus the hydraulic connection between aquifers appears to be maintained many months after the termination of the postseismic excursion (Figure 10) and the return of groundwater levels to the pre-seismic levels (Figures 4a and 4c).

5 Discussion

5.1 Postseismic Hydraulic Connectivity Between Wells

Before the earthquake, preexisting cracks in interlayered sediments are clogged by colloidal particles and precipitates; thus the aquitards are impermeable and the aquifers are hydraulically isolated (Figure 11a). Given the fact that overpressure was generated in the alluvial fan by the Chi-Chi earthquake as evidenced by water levels in wells (Figures 3 and 4) [*Chia et al*., 2008; *Wang et al*., 2001] and lasted ~2 months after the earthquake (Figures 3 and 4) and the fact that overpressure may hydrofracture clay-rich source beds, often more than several tens of meters thick, to allow oil or gas to flow out of the source beds, it may be reasonable to hypothesize that hydraulically conductive cracks were created in the aquitards after the Chi-Chi earthquake. Seismic shaking may also clear pre-existing cracks and create new ones to increase permeability in all directions (Figure 11b), with a magnitude similar to that of aquifers and several orders greater than the permeability in the vertical direction before the earthquake [e.g., *Wang et al.*, 2013]. The great increase in the vertical permeability causes postseismic convergence of water levels in clustered wells, as observed at many stations on the Choshui Alluvial Fan (Figures 3 and 4, and S1), and facilitates the hydraulic communication among aquifers, as evidenced by the similar postseismic tidal response of water level in wells at the Chuanhsin Station (Figures 7 and 8).

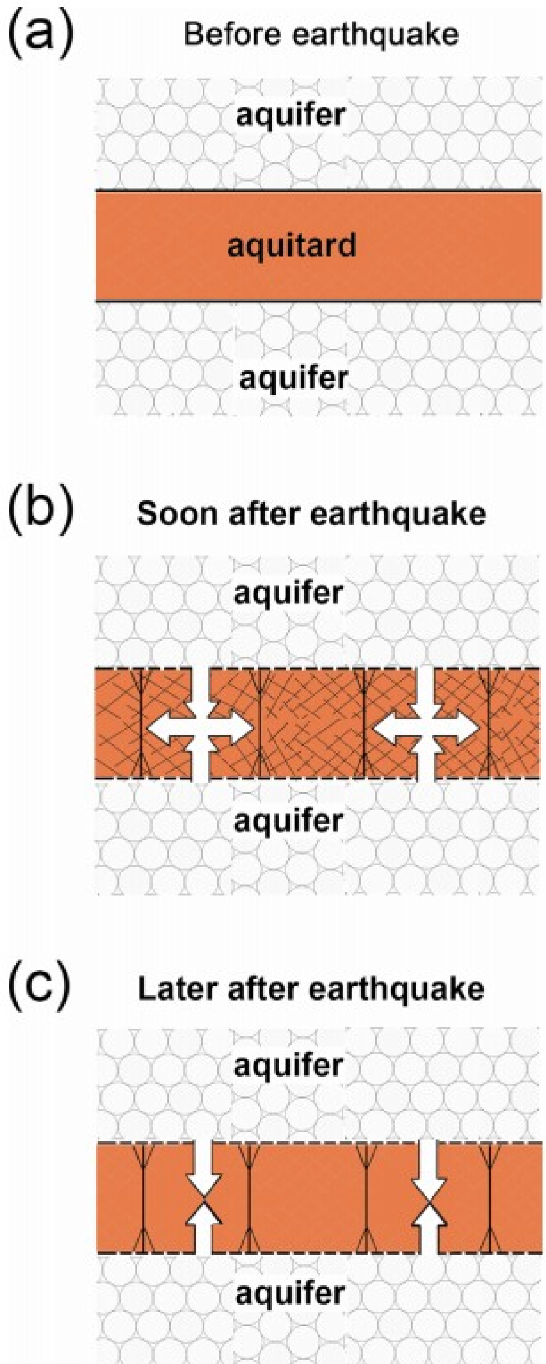

Figure 11. Conceptual model for the disruption of the groundwater system by earthquakes. (a) Before an earthquake the aquifers are hydraulically isolated from each other by an impermeable aquitard. (b) Earthquake creates some new cracks (shown by dark lines with branches) and clears preexisting cracks (shown by a network of thin lines), increasing permeability both along and across the aquitard. (c) Later after the earthquake, the preexisting cracks are reclogged, leaving only the newly formed cracks that continue to provide hydraulic communication between the aquifers.

The coseismic increase of the tidal amplitude (Figures 7 and 10) may partly be due to the undrained poroelastic response of the pressurized aquifer, i.e., undrained bulk modulus being greater than drained modulus. This mechanism, however, cannot explain the persistent increase of tidal amplitude during the month after the earthquake (Figures 7 and 10). We offer the following model to explain this continued, postseismic increase of tidal amplitude. Seismic shaking generates excess pore pressure not only in the aquifers but also likely in the aquitards. The increase in pore pressure decreases the effective pressure and softens the aquitard [*Seed and Lee*, 1966]; thus, a greater portion of the tidal load is transferred from the solid grains to the pore water. Since the bulk modulus of pore water is much greater than that of silty clays at low confining pressure [e.g., *Freeze and Cherry*, 1979], the bulk modulus of the aquitard and thus of the groundwater system increases after the earthquake. The increased bulk modulus causes the amplitude of the tidal pressure head (H) to increase (equation 4) and the tidal response to deviate from the trend of a confined aquifer (Figure 10). The increased pore pressure further weakens the sediments, causing more transfer of the tidal load from the solid grains to the pore water and a greater postseismic increase in H (Figure 10). This continues until the increase of pore pressure by load transfer is balanced by the dissipation of pore pressure due to lateral draining. After this, pore pressure decreases and sediments become stronger, until pore pressure reaches the preseismic level.

The increase of the tidal amplitude after the earthquake (Figures 7 and 10) cannot be caused by damage in the annular zone around the well bore because the thickness of the damaged zone (usually less than 0.1 m) is orders of magnitude smaller than the lateral extent of the water-level drawdown around the well under tidal loading (~100 m) [*Elkhoury et al*., 2006] and may not affect the tidal response [*Shi et al*., 2015]. Thus, the excursion in tidal response from the trend of a confined aquifer following the earthquake (Figure 10) can only be explained by increased vertical permeability in the aquitard between the aquifers, even if a hydraulic connection between the aquifers occurred adjacent to the well bore.

We also need to explain the continued hydraulic communication between aquifers (Figure 7) many months after the termination of the postseismic excursion (Figure 10) and the return of groundwater level to the preseismic level (Figure 4). One hypothesis is that while the seismically unclogged cracks in the aquitard may readily be reclogged by precipitates or colloidal particles [*Brodsky et al*., 2003], the newly formed cracks, with their clean and fresh surfaces, may be held open by irregular protrusions on the crack surface or by injection of fluidized sands into the crack and remain hydraulically conductive for much longer time (Figure 11c). The aquitard now would behave like a double porosity material, where the conductive cracks facilitate draining of pore water but have little storage or compressibility and the matrix is hydraulically impervious but stores most pore water. Because the compressibility of the cracks is negligible compared to that of unconsolidated sediments, the aquitard ceases to affect the amplitude of the tidal response of the wells, i.e., end of the excursions (Figure 10), even though the aquifers continue to be hydraulically connected afterward (Figure 7).

Another hypothesis is that the postseismic similarity in tidal response between different aquifers is due to hydraulic connectivity through a damage zone around the wells. In other words, the damaged zone with its high permeability may hydraulically connect the aquifers, resulting in a similar tidal response between the different aquifers. Field experiments may be needed to test which of the above hypotheses is more correct.

5.2 Why So Few Clustered Wells Show Water-Level Convergence and Tidal Evidence of Aquitard Breaching?

We did not find any correlation between the postseismic convergence of water levels with distance from the coast or from the epicenter (Figure 1), or with the lithology of the aquifers (Figure 2b), or with well depths (Figure 2b). Thus, we suggest that the breaching of aquitards may occur randomly by chance. Unconsolidated sediments are highly heterogeneous at the grain-scale, and during earthquakes hydraulically conductive cracks may extend by randomly connecting with other cracks. The chance for such an extending crack to cross an aquitard of tens of meters thick may be relatively low. This may explain in part why only ~10% of wells in the present study showed evidence of aquitard breaching. For tidal examination of the postseismic hydraulic connectivity between wells, an additional condition is required that the hydraulically connected wells show good tidal data. Wells installed in unconsolidated sediments, like those on the Choshui Alluvial Fan, usually have poor tidal response due to the relatively low bulk modulus of the sediments [e.g., *Roeloffs*, 1998]. This may explain why there was only one well cluster (i.e., the Chuanhsin Station) showing both postseismic convergence of water level and suitable data for tidal analysis.

5.3 Could Results of This Study Be Generalized to Other Geologic Settings?

Liao et al. [2015] studied the tidal response of water in a 4 km deep well drilled in consolidated sedimentary rocks before and after the 2008 M7.9 Wenchuan earthquake in China. The authors showed that there was both a coseismic increase in phase and a coseismic increase in the amplitude of the tidal response of water in the well, and interpret the latter to reflect a coseismic breaching of aquitards. Thus, coseismic breaching of aquitards may occur not only in unconsolidated alluvial fans but also in consolidated sedimentary rocks. In the latter case, the evidence for aquitard breaching lasted at least 2 years after the earthquake until the well was put out of service. Thus, the disruption of groundwater systems in consolidated rocks by large earthquakes can last for years.

5.4 What Would Be Needed to See If This Effect Is More Widespread?

Only one cluster of wells has suitable data for the kind of tidal analysis used in this study because of the simultaneous requirement of two conditions: first, the wells must show postseismic convergence of water levels and, second, the same wells must show good tidal responses. The first condition depends on the density of cracks generated by the earthquake, which in turn depends on, among other factors, the magnitude of and the proximity to the earthquake, which are difficult to control. The second condition depends on the mechanical property of the aquifers. As explained above, wells installed in unconsolidated sediments usually have poor tidal responses due to the relatively low bulk modulus of the sediments [e.g., *Roeloffs*, 1998]. Thus in order to document whether the responses reported in this study are common, we need more clustered wells installed in consolidated rocks in seismically active areas.

6 Summary

We show in this study that large earthquake can create vertical permeability in groundwater systems as high as that of aquifers by breaching the interlayered aquitards. In the following we summarize this study to answer the questions posed in the abstract: How do increases in the vertical permeability occur? How frequently do they occur? How long does the increased vertical permeability last after an earthquake? Is there a quantitative measure for monitoring and detecting the occurrence of aquitard breaching?

The disruption of groundwater systems by large earthquakes can last for years, at least for groundwater systems in consolidated rocks. The disruption may occur by breaching of aquitards as evident both by the post-seismic convergence of water levels (Figures 3 and 4) and by the deviation of the aquifer's tidal response on an amplitude-versus-phase diagram from the trend defined by a confined aquifer (Figure 10). We suggest that the latter, i.e., the deviation of the tidal response from the trend defined by a confined aquifer, may be a convenient and quantitative measure for continuous monitoring and detecting aquitard breaching.

We hypothesize that breaching of aquitards by large earthquakes is achieved by the formation of many hydraulically conductive cracks across the aquitards. The relatively small number of wells that showed evidence of aquitard breaching (~10%) may reflect the relative difficulty for cracks to connect across aquitards tens of meters thick. The change in the amplitude of tidal response of well water shows that the hydraulic connection between wells is due to increased vertical permeability across aquitards, not that along the damage zone adjacent to the well bore. The continued similarity in tidal response between wells long after the earthquake, on the other hand, could be caused either by conductive cracks breaching the aquitards or by a highly permeable damage zone around the well bore.

We can identify several ways to improve this model in future studies. First, the absence of ocean tide gauge data means that the detailed information of the tidal forcing is not available. Thus, we cannot derive from the tidal responses the poroelastic properties of the groundwater system before or after the earthquake but could only study the relative changes of aquifer properties. With better-constrained tidal loading, the long period changes in amplitude and phase (Figures 6 and 7) may be corrected and it will be possible to study the change of tidal response by earthquakes more quantitatively. Second, the model used here for interpreting tidal response is a model for horizontal flow in a confined aquifer; a model that accounts for the breached aquitard would add significantly more parameters, but might offer new insights into the changes especially if the detailed tidal loading was known. Third, the proposed model (Figure 11) predicts postseismic mixing of groundwater between the hydraulically connected aquifers and aquitards. Thus, some pore fluids in the aquitard will enter the aquifers and may leave a geochemical or isotopic signature in the aquifers, even though the volume of pore fluid contributed from the aquitard is expected to be very small. Finally, more clustered wells could be installed in consolidated rocks in seismically active areas in order to collect more data for the type of tidal response analysis in this study.

Breaching of aquitards by large earthquakes may be relevant to a number of societal issues in which confining layers are expected to protect the quality of water supplies and the safety of underground waste repositories. The result of this study, while specific for alluvial fans, may apply to different geologic settings. Thus, the method demonstrated here may be generally applicable to other seismically active areas.

Acknowledgments

Part of this paper is based on a talk given at the U.S. Geological Survey, Menlo Park, CA. We thank the Associate Editor and three anonymous reviewers for their comments that helped to improve the paper. We also thank Chi-Chao Huang for supplying the lithologic well logs in Figure 2b, and Chenchen Song for computing the power spectral density in Figure S5. The groundwater water level data of our study can be accessed through the following link: http://gweb.wra.gov.tw/hyis/. The study is partly supported by NSF EAR-1344424 and by the China Earthquake Administration Foundation for Young Teachers (20130102).

References

Agnew, D. C., and Y. Tamura (2008), Baytap08 user's manual, technical report, Scripps Inst. of Oceanogr. [Available at http://escholarship.org/uc/item/4c27740c.]

Briggs, R. O. (1991), Effects of Loma Prieta earthquake on surface waters in Waddell Valley, *Water Resour. Bull.*, 27, 991– 999.

Brodsky, E. E., E. Roeloffs, D. Woodcock, I. Gall, and M. Manga (2003), A mechanism for sustained groundwater pressure changes induced by distant earthquakes, *J. Geophys. Res.*, 108(B8), 2390, doi:10.1029/2002JB002321.

Chia, Y., J. J. Chiu, Y. H. Jiang, T. P. Lee, Y. M. Wu, and M. J. Horng (2008), Implications of coseismic groundwater level changes observed at multiple-well monitoring stations, *Geophys. J. Int.*, 172, 293– 301.

Cox, S. C., C. D. Menziers, R. Sutherland, P. H. Denys, C. Chamberlains, and D. A. H. Teagle (2015), Changes in hot spring temperature and hydrogeology of the Alpine Fault hanging wall, New Zealand, induced by distal South Island earthquakes, *Geofluids*, 15, 216– 239.

Elkhoury, J. E., E. E. Brodsky, and D. C. Agnew (2006), Seismic waves increase permeability, *Nature*, 411, 1135– 1138.

Fetter, C. W. (2001), *Applied Hydrogeology*, 4th ed., Prentice Hall, Upper Saddle River, N. J.

Freeze, R. A., and J. C. Cherry (1979), *Groundwater*, Prentice Hall, Englewood Cliff, N. J.

Hsieh, P., J. Bredehoeft, and J. Farr (1987), Determination of aquifer permeability from earthtide analysis, *Water Resour. Res.*, 23, 1824– 1832.

Ingebritsen, S. E., W. E. Sanford, and C. E. Neuzil (2006), *Groundwater in Geologic Processes*, 2nd ed., Cambridge Univ. Press, N. Y.

Ingebritsen, S. E., and C. E. Manning (2010), Permeability of the continental crust: Dynamic variations inferred from seismicity and metamorphism, *Geofluids*, 10, 193– 205, doi:10.1111/j.1468-8123.2010.00278.x.

Ingebritsen, S. E., D. R. Shelly, P. A. Hsieh, L. E. Clor, P. H. Seward, and W. C. Evens (2015), Hydrothermal response to a volcano-tectonic earthquake swarm, Lassen, California, *Geophys. Res. Lett.*, 42, 9223– 9230, doi:10.1002/2015GL065826.

Jan, S., C.-S. Chern, J. Wang, and S. Y. Chao (2004), The anomalous amplification of M2 tide in the Taiwan Strait, *Geophys. Res. Lett.*, 31, L07308, doi:10.1029/2003GL019373.

Jiang, C. Y., et al. (1999), Report of hydrogeological survey of Choshui Alluvial Fan, Taiwan—First master plan for groundwater monitor network [in Chinese], Water Resour. Bur., Ministry of Economic Affairs, Taiwan.

Lai, G., C. Jiang, L. Han, S. Sheng, and Y. Ma (2016), Co-seismic water level changes in response to multiple large earthquakes at the LGH well in Sichuan, China, *Tectonophysics*, 679, 211– 217.

Liao, X., C.-Y. Wang, and C. P. Liu (2015), Disruption of groundwater system by large earthquakes, *Geophys. Res. Lett.*, 42, 9758– 9763, doi:10.1002/2015GL066394.

Manga, M. (2001), Origin of postseismic streamflow changes inferred from baseflow recession and magnitude-distance relation, *Geophys. Res. Lett.*, 28, 2133– 2136.

Manga, M., and J. C. Rowland (2009), Response of alum rock springs to the October 30, 2007 earthquake and implication for increased discharge after earthquakes, *Geofluids*, 9, 237– 250.

Manga, M., E. E. Brodsky, and M. Boone (2003), Response of streamflow to multiple earthquakes and implications for the origin of postseismic discharge changes, *Geophys. Res. Lett.*, 30, 1214, doi:10.1029/2002GL016618.

Mogi, K., H. Mochizuki, and Y. Kurokawa (1989), Temperature changes in an artesian spring at Usami in the Izu Peninsula (Japan) and their relation to earthquakes, *Tectonophysics*, 159, 95– 108.

Mohr, C. H., M. Manga, C.-Y. Wang, J. W. Kirchner, and A. Bronstert (2015), Shaking water out of soil, *Geology*, 43, 207– 210.

Muir-Wood, R., and G. C. P. King (1993), Hydrological signatures of earthquake strain, *J. Geophys. Res.*, 98, 22,035– 22,068.

Roeloffs, E. A. (1998), Persistent water level changes in a well near Parkfield, California, due to local and distant earthquakes, *J. Geophys. Res.*, 103, 869–889.

Rojstaczer, S., and S. Wolf (1992), Permeability changes associated with large earthquakes: An example from Loma Prieta, California, 10/17/89 earthquake, *Geology*, 20, 211– 214.

Rojstaczer, S., S. Wolf, and R. Michel (1995), Permeability enhancement in the shallow crust as a cause of earthquake-induced hydrological changes, *Nature*, 373, 237– 239.

Seed, H. B., and K. L. Lee (1966), Liquefaction of saturated sediments under cyclic loading, *J. Soil Mech. Found. Eng. Am. Soc. Civ. Eng.*, 92, 105– 134.

Shi, Z., G. Wang, M. Manga, and C.-Y. Wang (2015), Mechanism of co-seismic water level change following four great earthquakes—Insights from co-seismic responses throughout the Chinese mainland, *Earth Planet. Sci. Lett.*, 430, 66– 74, doi:10.1016/j.epsl.2015.08.012.

Tamura, Y., T. Sato, M. Ooe, and M. Ishiguro (1991), A procedure for tidal analysis with a Bayesian information criterion, *Geophys. J. Int.*, 104, 507–516.

Wang, C.-Y. (2007), Liquefaction beyond the near field, *Seismol. Res. Lett.*, 78, 512– 517.

Wang, C.-Y., and M. Manga (2010), *Earthquakes and Water, Lecture Notes Earth Sci*., vol. 114, 249 pp., Springer, Berlin.

Wang, C.-Y., and M. Manga (2015), New streams and springs after the 2014 Mw6. 0 South Napa earthquake, *Nat. Commun.*, 6, 7597, doi:10.1038/ncomms8597.

Wang, C.-Y., L.-H. Cheng, C.-V. Chin, and S.-B. Yu (2001), Coseismic hydrologic response of an alluvial fan to the 1999 Chi-Chi earthquake, Taiwan, *Geology*, 29, 831– 834.

Wang, C.-Y., C. H. Wang, and M. Manga (2004a), Coseismic release of water from mountains: Evidence from the 1999 ($M_w = 7.5$) Chi-Chi, Taiwan, earthquake, *Geology*, 32, 769– 772.

Wang, C.-Y., M. Manga, D. Dreger, and A. Wong (2004b), Streamflow increase due to rupturing of hydrothermal reservoirs: Evidence from the 2003 San Simeon earthquake (2003), California, earthquake, *Geophys. Res. Lett.*, 31, L10502, doi:10.1029/2004GL020124.

Wang, C.-Y., C.-H. Wang, and C.-H. Kuo (2004c), Temporal change in groundwater level following the 1999 ($M_w = 7.5$) Chi-Chi earthquake (1999), Taiwan, *Geofluids*, 4, 210– 220.

Wang, C.-Y., L.-P. Wang, M. Michael, C.-H. Wang, and C.-H. Chen (2013), Basin-scale transport of heat and fluid induced by earthquakes, *Geophys. Res. Lett.*, 40, 3893– 3897, doi:10.1002/grl.50738.

Wang, H. F. (2000), *Theory of Linear Poroelasticity, Princeton Ser. Geophys*., Princeton Univ. Press, Princeton, N. J.

Xue, L., et al. (2013), Continuous permeability measurements record healing inside the Wenchuan earthquake fault zone, *Science*, 340, 1555– 1559, doi:10.1126/science.1237237.

Zahel, W. (1997), Ocean tides, in *Tidal Phenomena, Lecture Notes Earth Sci*., edited by H. Wilhelm, W. Zurn, and H.-G. Wenzel, vol. 66, pp. 113– 143, Springer, Berlin.